SEPTIEME COLLOQUE SUR LE TRAITEMENT DU SIGNAL ET SES APPLICATIONS

NICE du 28 MAI au 2 JUIN 1979

Système de Navigation de Précision pour Aterrissage d'Avions

A Navigation System for Air Traffic Precision Landing

JOSÉ MANUEL FONSECA DE MOURA

COMPLEXO I, INSTITUTO SUPERIOR TÉCNICO
AV. ROVISCO PAIS, 1000 LISBOA, PORTUGAL

RESUME

Pour quelques applications, il est nécessaire de develloper des systèmes de navigation pour aterrissage d'avions plus précise que les systèmes existant. La tour de controle de l'airport doit décider si l'avion est dans le correcte couloir d'aterrissage. Si non, elle directe l'avion à se préparer pour une nouvelle aterrissage.

Des erreurs de position résulte en conséquence de mesures incorrectes d'altitude et de vitesse. Des structures trop élevés ne peux pas être utilisés dans les airports. Des nouveaux radars actives introduit indésirable niveaux d'interference. Cette communication étudie un système passive de navigation d'aterrissage de précision. Il supose qu'il y a des senseurs passives placé aù long du couloir d'aterrissage, observant des signeaux de bande étroite emitté par l'avion. Le problème de location consiste à positioner l'avion rélativemment à ces senseurs. L'algorithm présenté a deux objectives: l'acquisition globale suivie par l'integration locale du mouvement de l'avion. La performance du système est étudié en fonction de la géometrie et du niveaux des bruits de la dynamique et d'observation.

SUMMARY

There is a need for improved accuracy in locating an airplane in three-dimensional space as it approaches landing. The airport control tower must decide whether the plane is following a nominal path leading to a safe landing. If not, it declares a missed approach, and the plane is directed to circle the airport to prepare for a new approach.An important source of location error derives from altitude and speed measurements, which may be affected by large inaccuracies. Very high structures cannot be used on an airport surface, and active systems may produce unacceptable interference problems. The paper investigates the feasibility of a precision landing monitor involving measurements of aircraft position by ground sensors.

It is supposed that there are passive antennas along the landing path monitoring narrow-band signals transmitted from the aircraft. The location problem is to position the plane with respect to these outriggers. The algorithm presented achieves the two main tasks: the global acquisition followed by the local tracking and integration of the dynamics. The system performance is studied by quantifying the tradeoffs between the errors and the signal to noise ratio and the geometric parameters assumed.

SYSTÈMES DE NAVIGATION DE PRÉCISION POUR ATERRISSAGE D'AVIONS

A NAVIGATION SYSTEM FOR AIR TRAFFIC PRECISION LANDING

1. PROBLEM DESCRIPTION

There is a need for improved accuracy in locating a plane in three-dimensional space as it approaches landing. The paper investigates the feasibility of a precision landing monitor involving passive measurements of aircraft position by ground sensors.

Figure 1 shows plan and side views for ideal landing geometry. At the left of both views is the runway, which is approached by the plane from the right. The aircraft course may be

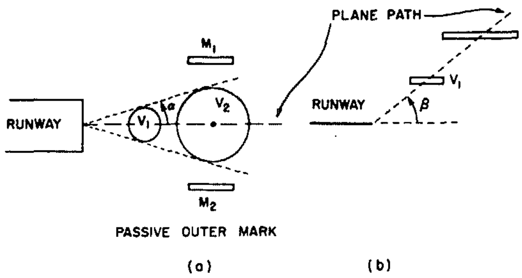

Plan View Side View

Figure 1: Landing Geometry

given by an azimuth α and an elevation angle β, both usually between 3^o and 6^o. To make a safe landing, the plane must follow a certain nominal path, defined at different ranges by shrinking cylindrical volumes $V_1, V_2, \ldots$, that measure the allowable error in the aircraft position (see circular sections on the side view of figure 1). At the threshold of the runway the plane's position should be known with a very small residual error.

It is assumed that there are passive antennas along the landing path monitoring narrow-band signals transmitted from the aircraft such as a single tone modulated by some coding for identification purposes. In order to avoid end-fire configurations, which lead to a considerable loss of performance, the passive structures are not placed at the end of the runway but are mounted along the approach path before the threshold of the runway, as indicated by outer marks M_1 and M_2 in figure 1. The passive location problem is to position the plane with respect to these outriggers.

The idealized version of this precision landing problem is sketched in figure 2. The aircraft position and dynamics are parametrized by the range R_O, the speed v with respect to the ground, and the two viewing angles θ_ℓ and θ_t.

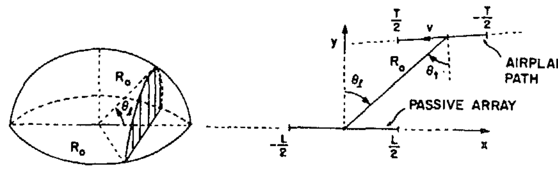

Figure 2: Precision Landing Geometry

The receiver has two main tasks: the global acquisition and the local tracking of the dynamics. For the global acquisition step the parameter vector

$$A = [R_o \;\; v \;\; \theta_t \;\; \theta_\ell]^T \qquad (1)$$

is modeled as nonrandom. The acquisition reduces to a 4-dimensional parameter nonlinear estimation problem. Maximum Likelihood (ML) techniques [1] are applied to derive the optimum receiver. The ML-processor involves a 4-dimensional maximization of the (log-) ML function. A two step, grid type algorithm, remnant of FSK-techniques, is used in [2], [3], [4], to implement this maximization.Therein, in section 2, the mean square error performance of the ML-receiver is investigated in the particular context of the air traffic precision landing scheme.

Once acquired,i.e.,the global geometry has been demodulated, the receiver has to follow the avionics motion. For this second task, the paper considers a different strategy: it describes the dynamics by a finite-dimensional system of stochastic differential equations. Within this framework, extended Kalman-Bucy filtering techniques are applied leading to a linearized recursive receiver that integrates the airplane dynamics.

Elsewhere [5], the receiver so presented is refered to as the hybrid algorithm for acquisition and tracking in platform location. It exhibits a decomposed structure, see figure 3: the nonlinear ML-processor,accomplishes the global acquisition of the platform, while the linearized, extended Kalman-Bucy filter (EKB) tracks the local dynamics.

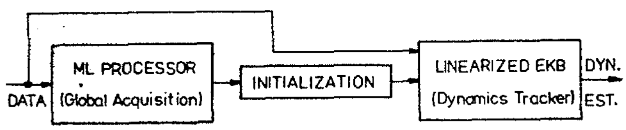

Fig. 3: Structure For The Receiver

SYSTÈMES DE NAVIGATION DE PRÉCISION POUR ATERRISSAGE D'AVIONS

A NAVIGATION SYSTEM FOR AIR TRAFFIC PRECISION LANDING

2. ACQUISITION MEAN SQUARE ERROR PERFORMANCE

As mentioned in section 1, inside the plane, a crystal radiates a single tone at frequency f that is observed to be corrupted by an additive, white, Gaussian noise. Because of the lack of synchronization, the phase of the received signal has a uniformly distributed random variable component (Rayleigh channel). The global acquisition step of the receiver fits the Maximum Likelihood parameter estimation framework [4].

For a jet plane in an airport traffic area, the altitude is below 10^4 ft, and the speed is required to be below maximum, taken here as approximately 200 knots. The speed measurement with respect to the ground may be in great error (depending on air circulation, wind speed, etc.); knowledge of the altitude may also be considerably inaccurate. In air traffic control the frequencies used are in the VHF or L-band. These considerations lead to the choice of numerical values indicated in table 1. Unless oftherwise stated, the nominal values listed are the ones assumed.

Frequency $f = 1GH_z$; wavelength $\lambda = 50$ ft			
Range $R_o < 10^4$ ft (typical $6x10^3$ ft)			
Speed v 200 knots (typical 300 ft/sec)			
$\theta_t = 15^o$; $\theta_\ell = 15^o$; Lin. Arr. Baseline L= 30ft			
Apriori	Range Uncertainty		$\Delta_M R_o < R_o/5$
"	Speed	"	Δ_M v < 80ft/sec
"	inclination	"	$\Delta_M \sin\theta_t = 1$
Observations Duration T= 8 sec;			
$X_t = vT/2R_o = .2$			

Table 1: Numerical Values for Precicion Landing

For these parameter values, the linear temporal baseline vT generated by the airplane is much larger than the outriggers antenna baseline. This means that the 4-dimensional search of the ML-receiver decouples in a 3-dimensional search for the actual parameter values of the reduced vector $A_o = [R_o \; v \; \theta_t]^T$, plus a one-dimensional search for the spatial bearing θ_ℓ, see [4]. The vector A_o is estimated from the temporal diversity of the received signals [3], while the bearing $\sin\theta_\ell$ is estimated from the relative delays across the receiving antennas (spatial diversity) [2]: the discussion is concerned with the tradeoffs and demands imposed by the range accuracy requirements on the geometric and statistical parameters. For the resulting signal-to-noise ratio values (SNR), the attainable accuracies for the other parameters are well within the desirable limits.

The total mean square error $\sigma^2_{tot_{A_j}}$ for parameter A_j at the output of the ML-processor is the sum of two components. One referred to as $\sigma^2_{g\ell_{A_j}}$, is associated with decision (or large errors) of the ML-processor (wrong choice of the grid cell). The other, $\sigma^2_{loc_{A_j}}$, is a local error resulting from the spread of the ML-ambiguity function. The local errors are estimated by the Cramer-Rao bounds $\sigma^2_{CR_{A_j}}$.

Figures 4 to 7 study the geometry and statistical tradeoffs. Figure 4 shows how the range accuracy changes with the signal to noise ratio SNR, for two values of the geometric parameter $X_t = VT/2R_o = 0.1, 0.2$, and two values of the region of uncertainty $\Delta_M R_o$. The linear aspect of all curves just reflect the modeling assumptions on the SNR dependence. For $X_t = .1$ the performance is well predicted by the Cramer-Rao bound. For $X_t = .2$, both the local and global errors contribute significantly to the mean-square performance: For this value of X_t the ML-algorithm exhibits, for the assumed geometry, a transitional behavior.

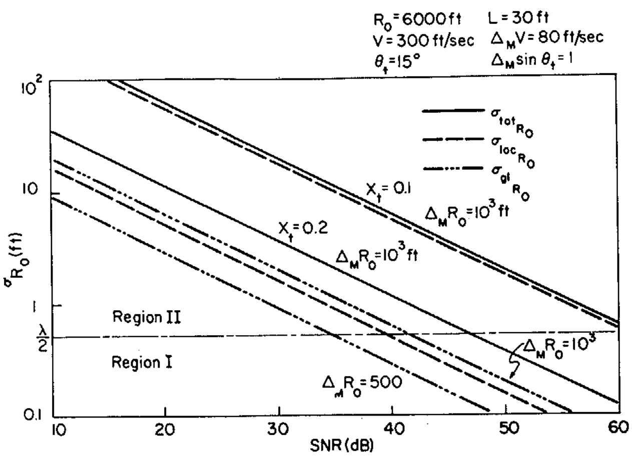

Figure 4: Range Accuracy vs SNR

Figure 5 shows the tradeoff between required SNR and actual aircraft-passive receiver separation, for two typical accuracy requirements, $\sigma_{R_O} = \lambda/2$ ft, $\sigma_{R_O} = 50$ ft.

Note the extra 40 dB required to go from region II (called tracking within geometry) to region I (called tracking within phase). The large a priori uncertainty, inducing significant global error, is responsible for the additional SNR required with respect to the value predicted by the Cramer-Rao bound. Figure 4 suggests an itterative global acquisition scheme, where several pairs of receiving elements are placed along the airplane landing path, with increasingly greater accuracy requirements. This strategy is in accordance with the vanishing sequence of uncertainty cylinders of figure 1. As the plane travels through, $\Delta_M R_O$ is reduced from one iteration to the next, with the net effect of diminishing $\sigma_{g\ell_{R_O}}$ and leading to a performance which approaches the Cramer-Rao bounds.

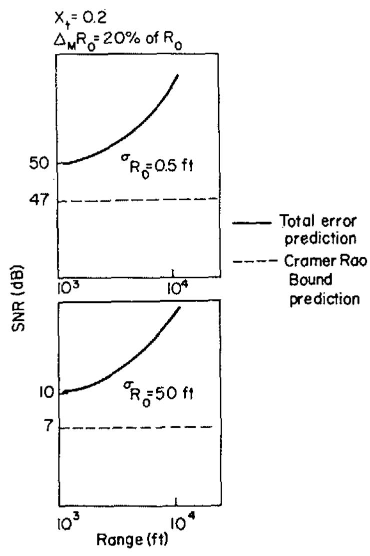

Fig. 5: SNR vs Range

Figure 6 studies as a function of the separation R_O the total acquisition time T_{acq} necessary for the receiver to attain the two given accuracy requirements. The linearity of the lower curve (tracking within the geometry) reflects the linear dependence of the Cramer-Rao on T_{acq}. The tracking within phase (upper curve) changes from the Cramer--Rao dependence to a global dependence, with a sharper slope. Since limitations imposed by path random perturbations restrict the increase of the acquisition interval, figure 6 says that if the overall geometry does not lead to a Cramer-Rao dependence, it is unrealistic to expect to improve the estimation accuracy significantly by simply increasing the acquisition time: higher performance standards have to be met with enough SNR.

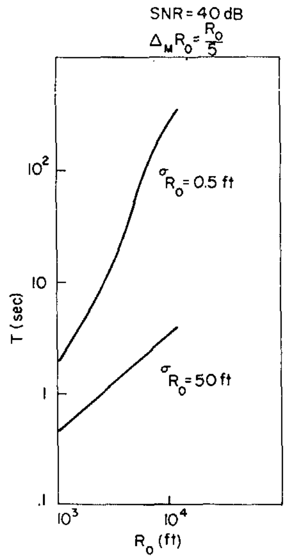

Fig. 6: T_{acq} vs Range

Figure 7 studies the speed accuracy versus SNR, for two different mean-square speed accuracies. It is apparent that for slower avionics the total temporal baseline is shorter, hence leading to a deterioration of performance (left end of both curves). This can be partly compensated by increasing T_{acq}, depending on the path perturbation (see comments above). Even for $\sigma_V = .1$ ft/sec, which may be thought of as an upper bound on the desired speed accuracy in most practical situations, the necessary SNR is less than 50 dB, which is below the SNR demanded by the tracking within the phase acquisition mode.

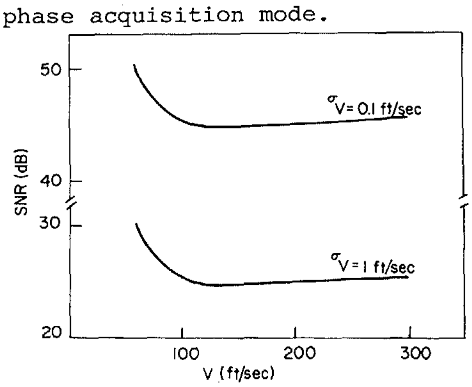

Fig. 7: SNR/Aircraft Speed

SYSTÈME DE NAVIGATION DE PRÉCISION POUR ATERRISSAGE D'AVIONS

A NAVIGATION SYSTEM FOR AIR TRAFFIC PRECISION LANDING

3. RELATED HYBRID ALGORITHM ISSUES

In the context of the precision landing scheme, one has still to consider the sensitivity of the ML-algorithm to path disturbances, and the extended Kalman-Bucy linear tracker of figure 3. If Q represents the noise power level of the random path perturbations, T_{acq}, the total (acquisition) time used by the ML-receiver, and Σ_R the mean square range error induced by the path variations, table 2 summarizes, for several Q and T, the path induced standard deviation errors. It shows that the

$\Sigma_R^{1/2}$ (ft)	.004	.4	20	$Q(ft^2/sec^3)$
4	.15	1.45	10	
8	.35	4.12	30	
T_{acq}(sec)				

Table 2: Path Variation Errors

path variations may be a limiting factor on the final attainable accuracy.

The source parameter estimates returned by the ML-processor serve to initialize the extended Kalman-Bucy (EKB) tracker. It can be shown that, for a low SNR=10 dB (in terms of the precision landing application) and Q=1, the asymptotic EKB mean square error perfomance is $\sigma^2_{EKB_R} \cong .367\ ft^2$ and $\sigma^2_{EKB_{\dot{R}}} \cong .365^2\ (ft/sec)^2$. These numbers mean that no significant degradation is introduced by the EKB during the observation interval.

4. CONCLUSION

The preceding analysis shows that the range global acquisition is the determining factor of the receiver's performance in the passive precision landing scheme just studied. There are two main sources of inaccuracy: errors incurred by the ML-receiver, because of the additive noise disturbances, and errors induced by flight turbulence.

A practical solution to the passive precision landing, with two sets of passive outriggers, is illustrated in figure 8.

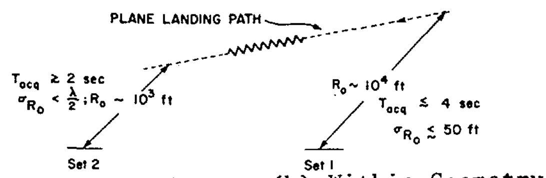

(a) Within Phase (b) Within Geometry

Fig. 8: Passive Tracking Solution

Relatively early in the approach path is placed a passive receiving element (set 1) designed for tracking planes at 10^4 feet range with 300 ft/second speed. Between set 1 and set 2 the plane is recursively tracked by the EKB. Set 2 is placed deeper in the landing path, being designed to track planes at 10^3 ft range, with nominal speeds of 150 ft/sec. From then on, the plane is tracked by the EKB. Assuming the nominal values of table 1, SNR=50 dB, and that the receiver elements in each set have L=50 feet, figure 9 studies the attainable range accuracies for light ($\sqrt{Q_2}=g/10$) and medium ($\sqrt{Q_1}=g/2$) turbulence flight conditions (here $g \cong 32\ ft/sec^2$ is the gravitational constant).

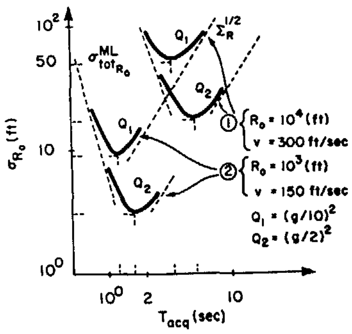

Fig. 9: Range Accuracy vs T_{acq}

The upper curves in figure 9 correspond to the expected perfomance at set 1 of the outriggers in figure 8, while the lower curves, to set 2. For the indicated turbulence conditions, the range acquisition accuracy depends on both the ML receiver perfomance $\sigma^{ML}_{tot_{R_0}}$ and the root mean square path variance, which limits the maximum acquisition time and attainable accuracy.

BIBLIOGRAPHY

[1] - H.L. Van Trees, "Detection, Estimation and Modulation Theory: Part III", New York: Wiley, 1971.

[2]- José M. F. Moura and Arthur B. Baggeroer, "Passive Systems Theory with Narrow-Band and Linear Constraints: Part I - Spatial Diversity", IEEE Journal of Oceanic Enginneering, Vol. OE-3, No. 1,Jan,1978, pp. 5-13.

[3]- José M. F. Moura, "Passive Systems Theory With Narrow-Band and Linear Constraints: Part II - Temporal Diversity", IEEE Journal of Oceanic Engineering, Vol.OE-4, No. 1, Jan, 1979.

[4]- José M. F. Moura, "Passive Systems Theory with Narrow-Band and Linear Constraints: Part III - Spatial/Temporal Diversity", submitted for publication.

[5]- José M. F. Moura, "The Hybrid Algorithm: A Solution to Acquisition and Tracking in Platform Location", to be submitted for publication.